ACS OMEGA

http://pubs.acs.org/journal/acsodf

Article

Simple Approach for Fluorescence Signal Amplification Utilizing a Poly(vinyl alcohol)-Based Polymer Structure in a Microchannel

Keine Nishiyama, Masatoshi Maeki, Akihiko Ishida, Hirofumi Tani, Hideaki Hisamoto, and Manabu Tokeshi*

Cite This: *ACS Omega* 2021, 6, 8340−8345

Read Online

ACCESS | Metrics & More | Article Recommendations | Supporting Information

ABSTRACT: Analytical methods with fluorescence detection are in widespread use for detecting low abundance analytes. Here, we report a simple method for fluorescence signal amplification utilizing a structure of an azide-unit pendant water-soluble photopolymer (AWP) in a microchannel. The AWP is a poly(vinyl alcohol)-based photocross-linkable polymer, which is often used in biosensors. We determined that the wall-like structure of the AWP (AWP-wall) constructed in a microchannel functioned as an amplifier of a fluorescence signal. When a solution of fluorescent molecules was introduced into the microchannel having the AWP-wall, the fluorescent molecules accumulated inside the AWP-wall by diffusion. Consequently, the fluorescence intensity inside the AWP-wall increased locally. Among the fluorescent molecules considered in this paper, 9*H*-(1,3-dichloro-9,9-dimethylacridin-2-one-7-yl) (DDAO) showed the highest efficiency of fluorescence signal amplification. We prepared a calibration curve for DDAO using the fluorescence intensity inside the AWP-wall, and the sensitivity was 5-fold that for the microchannel without the AWP-wall. This method realizes the improved sensitivity of fluorescence detection easily because the fluorescence signal was amplified only by injecting the solution into the microchannel having the AWP-wall. Furthermore, since this method is not limited to only the use of microchannel, we expect it to be applicable in various fields.

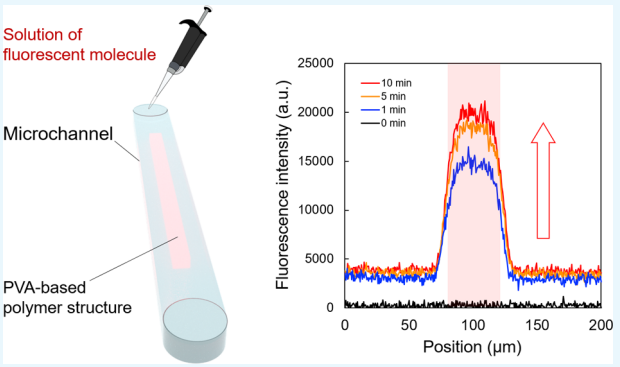

INTRODUCTION

A lot of efforts have been put into detecting trace amounts of analytes in complex samples like biological materials in recent years, and the detection of trace amounts of biomarkers in body fluids has attracted attention for the early diagnosis of serious diseases.[1,2] For example, there are demands for the sensitive detection (∼ng/mL level) of cancer biomarkers such as prostate-specific antigen and carcinoembryonic antigen.[3,4] To meet these demands, various detection methods for biomarkers using microfluidic devices have been reported.[5−8] Microfluidic devices are useful tools for miniaturized detection systems. However, it remains challenging to achieve both high sensitivity and construction of an easy-to-use and rapid detection system.

For point-of-care testing with protein biomarkers, we have previously developed a microfluidic device (immuno-wall device) for a highly sensitive immunoassay.[9−12] Capture antibodies were immobilized on the wall-like structure made from an azide-unit pendant water-soluble photopolymer (AWP-wall) in a microfluidic channel. A sandwich immunoassay was performed by pipette operations, and all reactions for the immunoassay were completed in an incubation time of several tens of minutes. At the same time, we found a phenomenon in which the fluorescence signal increased locally inside the AWP-wall. This property was combined with an enzymatic reaction, which resulted in significant improvement in detection sensitivity of the immuno-wall device.[10] Since the fluorescence signal was amplified only by injecting the solution into the microchannel having the AWP structure, the process of signal amplification was simple. However, the characteristics and mechanism of the AWP-wall as a fluorescence signal amplifier have not been discussed. Clarifying these issues is important for constructing a better method of signal amplification.

Here, we report that the AWP-wall in the microchannel plays a role of an amplifier of the fluorescence signal. Our proposed method was based on the spontaneous concentration by the accumulation of fluorescent molecules in the AWP-wall. Typical concentration methods of molecules with microdevices include using liquid−liquid extraction,[13,14] nanoporous membranes,[15,16] and electrophoresis.[17,18] Although the concen-

Received: January 5, 2021
Accepted: March 9, 2021
Published: March 17, 2021

https://doi.org/10.1021/acsomega.1c00057
ACS Omega 2021, 6, 8340−8345

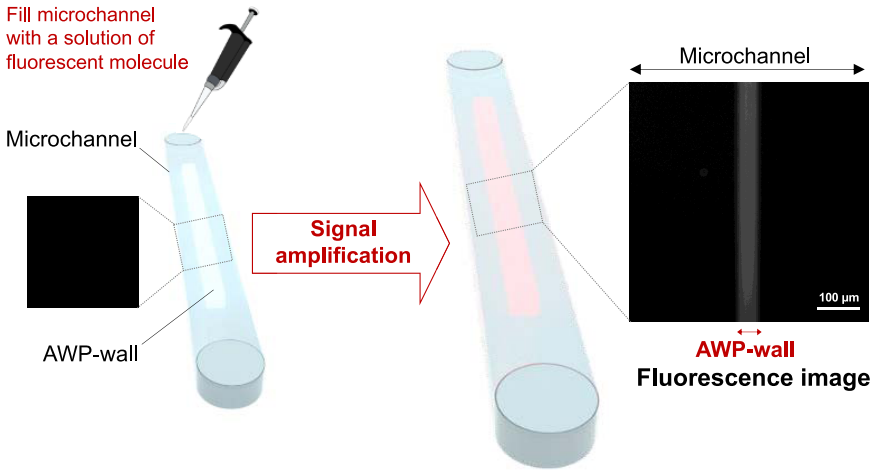

Figure 1. Schematic illustration of fluorescence signal amplification by the AWP-wall. The right inset photo is the fluorescence image of the AWP-wall in a microchannel after the injection of 1 μM 9*H*-(1,3-dichloro-9,9-dimethylacridin-2-one-7-yl) (DDAO).

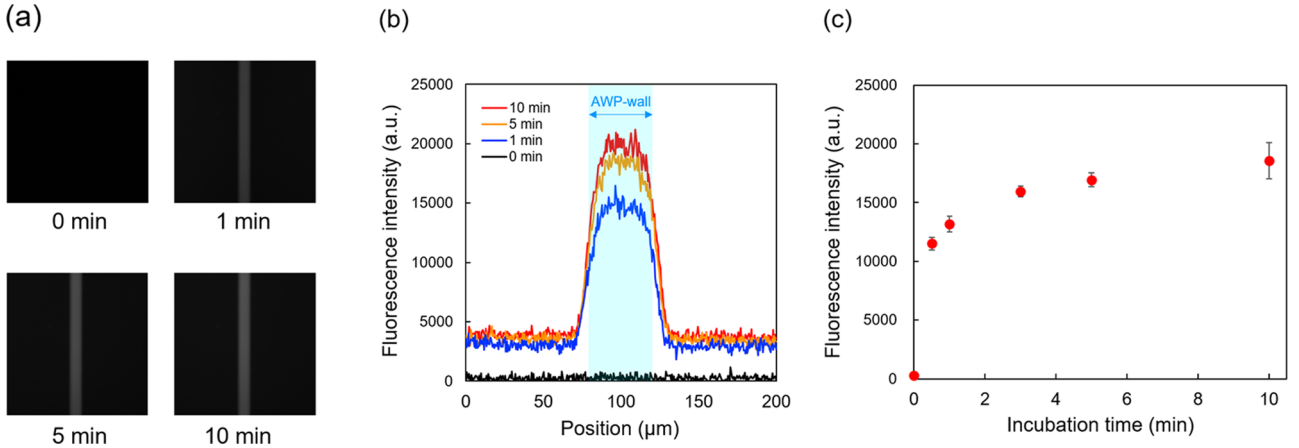

Figure 2. Fluorescence signal amplification of DDAO by the AWP-wall. DDAO (1 μM) was injected into a microchannel and incubated for 10 min. The time in this figure refers to incubation time. (a) Fluorescence image of the AWP-wall in the microchannel. (b) Fluorescence intensity profile as a function of the position around the AWP-wall. (c) Fluorescence intensity inside the AWP-wall as a function of incubation time.

tration efficiency of these methods is high, expensive external equipment and complicated operations are required for the concentration. In our proposed method, fluorescence signal amplification was accomplished without external equipment or additional operations (Figure 1). This feature is a great advantage for analytical systems that required simplicity and rapidness. We describe our work to characterize the AWP-wall as a fluorescence signal amplifier in the microchannel and we elucidate the mechanism of fluorescence signal amplification.

■ RESULTS AND DISCUSSION

The AWP-wall (40 μm × 4 mm × 40 μm) was fabricated in a microchannel as a simple model of the fluorescence signal amplification by an AWP structure (Figure S1). In our previous work, we found high fluorescence intensity locally inside the AWP-wall when alkaline phosphatase reacted with 9*H*-(1,3-dichloro-9,9-dimethylacridin-2-one-7-yl) phosphate (DDAO phosphate) outside the AWP-wall.[10] Therefore, we first investigated the fluorescence signal amplification by the AWP-wall using DDAO, which is a fluorescent species formed as a product of the enzymatic reaction from DDAO phosphate. A 1 μM DDAO solution was injected into the microchannel having the AWP-wall, and fluorescence intensity around the AWP-wall was measured (Figure 2). Figure 2a,b shows that the fluorescence intensity inside the AWP-wall was high locally at 1 min after the solution injection. Additionally, the fluorescence intensity inside the AWP-wall increased over time and reached a plateau at 10 min after the DDAO injection. We clarified that the AWP-wall worked as a fluorescence signal amplifier even if DDAO was introduced into the microchannel having the AWP-wall.

Next, we investigated the dependence of the DDAO concentration on the fluorescence intensity inside the AWP-wall. The calibration curves of DDAO were prepared using the fluorescence intensity inside and outside the AWP-wall to compare both sensitivities (Figure 3). The average value of the fluorescence intensity of each pixel inside the AWP-wall was denoted as I_{wall}, and that outside the AWP-wall was denoted as $I_{channel}$ (Figure 3a). Figure 3b shows calibration curves with I_{wall} and $I_{channel}$. I_{wall} and $I_{channel}$ increased linearly as the DDAO concentration increased. The slope of the calibration curve using I_{wall} was about 5 times that of $I_{channel}$ (Figure 3b). The limit of detection (LOD) of DDAO was 2.7 nM when using I_{wall}. From the above results, we found that I_{wall} was dependent on the DDAO concentration and it could be used for the highly sensitive detection of DDAO.

https://doi.org/10.1021/acsomega.1c00057
ACS Omega 2021, 6, 8340−8345

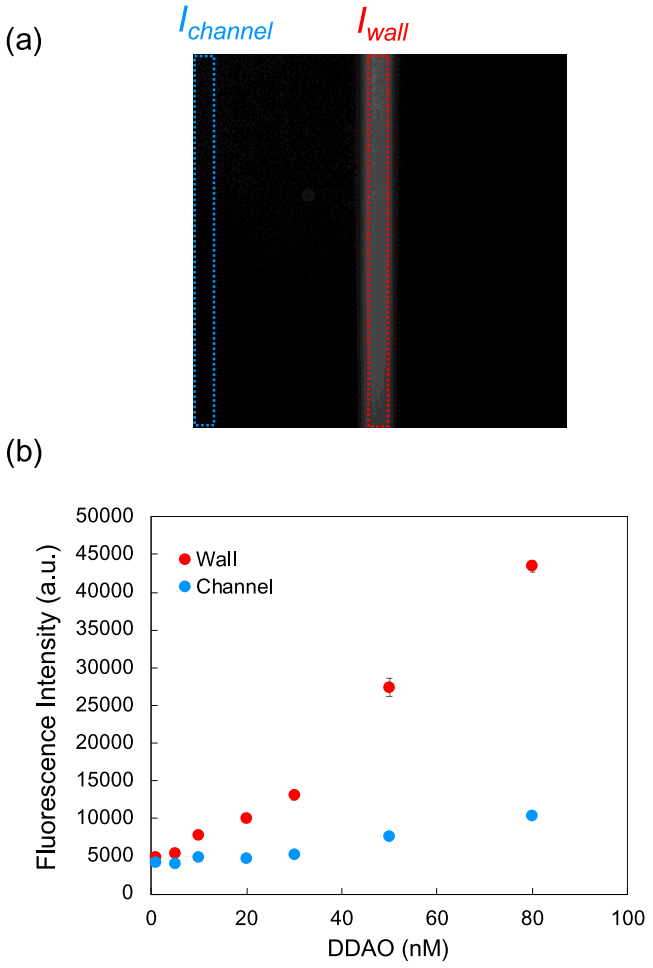

Figure 3. (a) Photograph of the fluorescence image of the AWP-wall in a microchannel after injection of 1 μM DDAO. The red dotted rectangle represents the detection area of the AWP-wall. The blue one represents the detection area of the microchannel. (b) Calibration curves of DDAO with different detection areas. The plot of the lowest DDAO concentration was 1 nM. Incubation time: 10 min.

The increase in the fluorescence intensity of DDAO inside the AWP-wall was presumably due to one or both of the following two factors. The first factor is the increment of the fluorescence quantum yield of DDAO in the AWP environment. The second one is the accumulation of DDAO inside the AWP-wall. At first, to discuss the possibility of increasing the fluorescence quantum yield of DDAO in the AWP, we obtained the fluorescence spectrum of a mixture of the AWP and the DDAO solution (Figure 4). After thoroughly mixing the AWP and DDAO, the mixture was irradiated with UV light to polymerize it, and then the fluorescence spectrum was measured. When the AWP percentage in the mixture was 10% or less, there were almost no changes in the fluorescence peak wavelength and fluorescence intensity. When the AWP percentage was 50% (the same as in the AWP-wall), the fluorescence intensity increased and the fluorescence peak wavelength shifted slightly from 658 to 662 nm. Although there are few reports available on the fluorescence quantum yield of DDAO, Gong et al.[19] reported that the fluorescence intensity of DDAO was enhanced by Triton X-100 (a nonionic surfactant). We inferred from these data that the hydrophobic domain of the AWP might lead to an increase in the fluorescence quantum yield of DDAO. However, since the

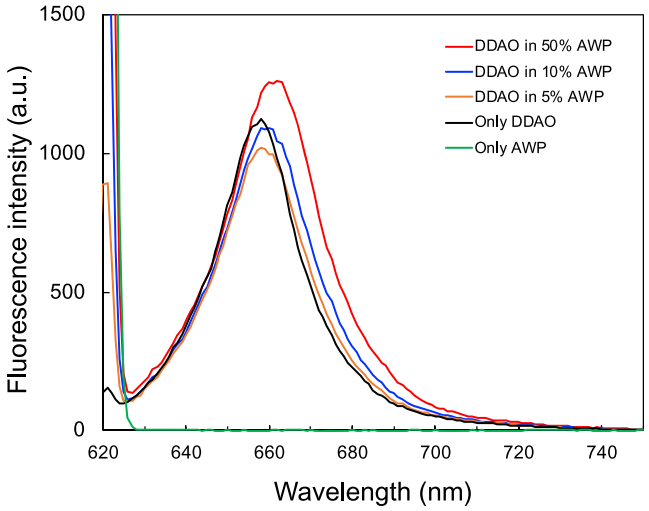

Figure 4. Fluorescence emission spectra of 5 μM DDAO in the mixture of Tris−HCl buffer (pH 8.0) and the AWP.

increase in the fluorescence intensity was small, the change in the fluorescence quantum yield of DDAO in the AWP was judged to make a trivial contribution to the fluorescence signal amplification by the AWP-wall.

To discuss the accumulation of fluorescent molecules in the AWP-wall, we compared the efficiency of fluorescence signal amplification by the AWP-wall with four fluorescent molecule species in addition to DDAO (Figure 5). The AWP has a peak absorption wavelength at ∼310 nm, and the autofluorescence of the AWP could be significantly reduced by using long-wavelength excitation light.[10] Therefore, we selected fluorescent molecules (DDAO, Alexa Fluor 647, ATTO 647N, Cy5) that emit far-red fluorescence and Cy3, which has a structure similar to Cy5 and emits greenish yellow fluorescence. The chemical structures of these species are shown in Figure S2. Tris−HCl buffer containing each of the fluorescent species individually was introduced into a microchannel having the AWP-wall, and I_{wall} and $I_{channel}$ were obtained over time. The efficiency of the fluorescence signal amplification of the AWP-wall was defined as $I_{wall}/I_{channel}$. $I_{wall}/I_{channel}$ increased over time for all fluorescent molecule species studied, and the fluorescence signal was amplified in the AWP-wall ($I_{wall}/I_{channel} > 1$) (Figure 5a,b). Because I_{wall} of each species increased gradually over time, we assumed that these fluorescent molecules were accumulated inside the AWP-wall by diffusion. Additionally, we clarified that the amplification of the fluorescence signal by the AWP-wall was not a phenomenon specific to DDAO, although DDAO showed the highest $I_{wall}/I_{channel}$ at 10 min after injection (Figure 5c).

Then, we focused on the properties of fluorescent molecules and the AWP to discuss their interactions. The AWP is a polymer based on poly(vinyl alcohol) (PVA) (Figure S3).[20] Baptista et al.[21] presented a molecular dynamics simulation showing that highly hydrophobic molecules interact with PVA through hydrophobic interactions and hydrogen bonds. There is also a possibility that the molecular size influences the ability of a molecule to penetrate the AWP-wall. To consider these contributions, we looked at the effects of the octanol−water partition coefficient ($\log P$) and the molecular weight of each fluorescent molecule on $I_{wall}/I_{channel}$ and this is shown in Figure S4. DDAO had the highest $\log P$ and the lowest molecular weight among the fluorescent molecules we considered.

https://doi.org/10.1021/acsomega.1c00057
ACS Omega 2021, 6, 8340−8345

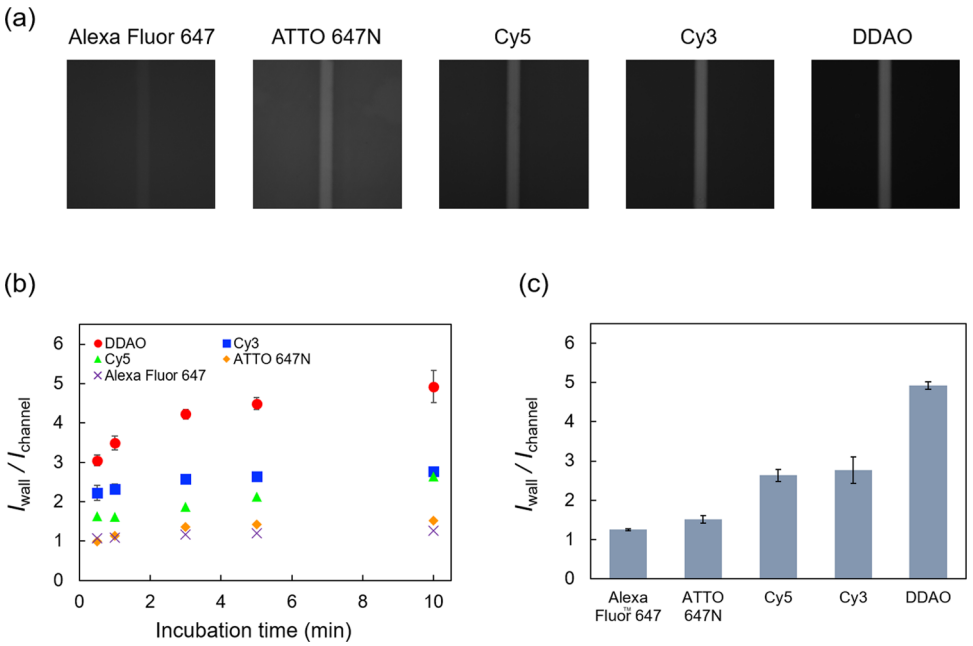

Figure 5. Evaluation of the AWP-wall as a fluorescence signal amplifier with five different fluorescent molecules. The concentration of each fluorescent species was 1 μM. (a) Fluorescence images of the AWP-wall after injecting the solution of fluorescent molecules. Incubation time: 10 min. (b) $I_{wall}/I_{channel}$ as a function of time. (c) Comparison of $I_{wall}/I_{channel}$ among fluorescent molecules. Incubation time: 10 min.

Besides, there seemed to be a positive correlation between log P (Figure S4a) and $I_{wall}/I_{channel}$, and a negative correlation between the molecular weight and $I_{wall}/I_{channel}$ (Figure S4b). We can deduce that hydrophobicity and low molecular weight enhance the accumulation of fluorescent molecules in the AWP-wall, which leads to the high efficiency of signal amplification. Moreover, Chang et al.[22] suggested that the nitrogen atom of the pyridine moiety showed a strong intermolecular interaction with PVA because of their electrostatic interactions and hydrogen bonding. The nitrogen atom in DDAO may lead to a strong intermolecular interaction with the AWP.

Lastly, the accumulation behavior of fluorescent molecules in the AWP was investigated using another platform (Figure S5). A sample solution of fluorescent molecules was introduced into a well of a microplate having a polymerized AWP on the bottom and the solution was incubated for 2 h. Then, a portion of the supernatant was transferred to an empty well and its fluorescence intensity was measured (Figure S5a). By measuring the fluorescence intensity of the supernatant, we were able to ignore the effect of the AWP environment on the fluorescence quantum yield of fluorescent molecules. As indicated in Figure S5b, the fluorescence intensity of the supernatant after incubation decreased compared to the control containing all of the fluorescent molecules. The amount of change in the fluorescence intensity of DDAO was the highest. These results support our hypothesis that the accumulation of fluorescent molecules in the AWP contributes to fluorescence signal amplification by the AWP-wall. We found that the fluorescent molecules were accumulated in the AWP even when it was as an AWP-wall in a microplate well. Thus, our proposed method has good potential for extending its applications to various fields.

CONCLUSIONS

We determined that the AWP-wall in the microchannel functioned as a fluorescent signal amplifier. Among the five fluorescent molecule species we considered, DDAO showed the highest efficiency of fluorescence signal amplification. The calibration curve of DDAO using the fluorescence intensity inside the AWP-wall had about 5 times the sensitivity compared to that outside the AWP-wall. The accumulation of fluorescent molecules inside the AWP-wall contributed to the fluorescence signal amplification. Also, the high specific surface area of the AWP-wall enabled the rapid accumulation of fluorescent molecules in the AWP-wall.

This method does not require expensive external equipment and complicated operations to concentrate the molecules. Fluorescence signal amplification is accomplished simply by injecting a solution into a microchannel having the AWP-wall. Therefore, this method could be a new component technology for developing a simple analytical method. We expect this method to be utilized for detecting low abundance analytes. For example, DDAO phosphate and DDAO galactoside are widely used as fluorogenic substrates for enzymatic reactions. Therefore, by combining these substrates with fluorescence signal amplification by the AWP-wall, a highly sensitive detection method can be devised. Moreover, since this method is not limited to use in a microchannel, it has widespread applicability.

EXPERIMENTAL SECTION

Materials. Hydrochloric acid was purchased from FUJIFILM Wako Pure Chemical Corporation (Japan). Trizma base was purchased from Sigma-Aldrich Co. LLC. A phosphate-buffered saline (PBS; pH 7.4) solution and Alexa Fluor 647 carboxylic acid were purchased from Thermo Fisher Scientific, Inc. ATTO 647N free COOH was purchased from Atto-Tec GmbH (Germany). Cy3 carboxylic acid and Cy5 carboxylic acid were purchased from Lumiprobe Corporation. DDAO

https://doi.org/10.1021/acsomega.1c00057
ACS Omega 2021, 6, 8340−8345

was purchased from Santa Cruz Biotechnology, Inc. An azide-unit pendant water-soluble photopolymer (AWP, 6%) was purchased from Toyo Gosei Co., Ltd. (Japan).

AWP-Wall in a Microchannel. The AWP-wall in a microchannel was fabricated in accordance with the literature with slight modifications.[10] In short, we used a microchip having 40 straight microchannels, which was made from a cyclic olefin copolymer (Sumitomo Bakelite Co., Ltd., Japan). A microchannel was filled with a mixture of AWP and PBS (volume ratio 1:1). Then, the UV light from a mercury lamp (Hayashi Watch Works LA-410 UV) was irradiated onto the mixture in the microchannel through the photomask for 8 s. Subsequently, the uncured AWP was removed by a vacuum pump (SP 20, Air Liquide Medical Systems, France) and washed with PBS to reveal the resulting structure (AWP-wall). Figure S1 shows the photograph and schematic illustration of the microchip and the AWP-wall.

Evaluation of the AWP-Wall in a Microchannel as a Fluorescence Signal Amplifier. The fluorescent molecule species (DDAO, Alexa Fluor 647, ATTO 647N, Cy5, or Cy3) in 1 M Tris−HCl buffer (pH 8.0) was injected into the microchannel having the AWP-wall quickly (∼0.5 s). After a certain incubation time, the fluorescence image of the microchannel was captured without removing the solution with an inverted fluorescence microscope (Keyence BZ-9000). Two filter cubes of the fluorescence microscope were used: TRITC filter (Keyence OP-66837; excitation 540/25 nm, emission 605/55 nm) for Cy3 and Cy5 filter (Keyence OP-87766; excitation 620/60 nm, emission 700/75 nm) for DDAO, Alexa Fluor 647, ATTO 647N, and Cy5. The exposure time of the microscope was adjusted appropriately according to each experiment. The fluorescence image was analyzed with ImageJ software to calculate the fluorescence intensity. The fluorescence intensity was calculated as the average value of the fluorescence signals from all pixels in the selected area.

Evaluation of the Transfer of Fluorescent Molecules to the AWP in a Microplate. The AWP (50 μL) was injected into a well in a 96-well microplate (Thermo Fisher Scientific Nunc F96 MicroWell Black Polystyrene Plate). Then, the UV light from a mercury lamp (Hayashi Watch Works LA-410 UV) was irradiated onto the microplate for 16 s. Subsequently, the 1 μM concentration of fluorescent molecule species (DDAO, Alexa Fluor 647, ATTO 647N, Cy5, or Cy3) in 1 M Tris−HCl buffer (pH 8.0, 200 μL) was injected into the microplate containing the AWP. After 2 h incubation, 100 μL of the supernatant liquid in the well was moved to an empty well (∼10 μL of a solution of fluorescent molecules was absorbed into the AWP). The fluorescence intensity of this supernatant liquid was measured with a microplate reader (Tecan Infinite 200 PRO). The excitation filter at 620/20 nm and the emission filter at 670/25 nm were used for DDAO, Alexa Fluor 647, ATTO 647N, and Cy5. The excitation filter at 540/25 nm and the emission filter at 590/20 nm were used for Cy3.

Fluorescence Spectrum of DDAO. The AWP was added to DDAO in 1 M Tris−HCl buffer (pH 8.0). The final concentration of DDAO in the mixture was 5 μM and that of the AWP was adjusted to 5, 10, or 50% (v/v). After the mixing of the DDAO solution and the AWP by a vortex mixer (Scientific Industries Vortex-Genie 2), the mixture (3 mL) was added into a disposable poly(methyl methacrylate) cell (Kartell, Italy). Then, the UV light from the mercury lamp was irradiated onto the mixture for 16 s. The fluorescence emission spectrum of the cured mixture was measured by a fluorescence spectrophotometer (Hitachi F-7000). The excitation wavelength was 620 nm.

Prediction of the Octanol−Water Partition Coefficient. The octanol−water partition coefficient (log P) of the fluorescent molecules was calculated by Swiss ADME predictor software (http://www.swissadme.ch/). This software predicts log P by combining the generalized Born and solvent accessible surface area models into a method known as the iLogP method.[23]

■ ASSOCIATED CONTENT

Supporting Information

The Supporting Information is available free of charge at https://pubs.acs.org/doi/10.1021/acsomega.1c00057.

Photograph and design of the microchip; chemical structures of fluorescent molecules; chemical structure of the AWP; correlations of $I_{wall}/I_{channel}$ with log P and molecular weight; and evaluation of the transfer of fluorescent molecules to the cured AWP in a microplate (PDF)

■ AUTHOR INFORMATION

Corresponding Author

Manabu Tokeshi − *Division of Applied Chemistry, Faculty of Engineering, Hokkaido University, Sapporo 060-8628, Japan; Innovative Research Centre for Preventive Medical Engineering, Nagoya University, Nagoya 464-8601, Japan; Institute of Innovation for Future Society, Nagoya University, Nagoya 464-8601, Japan;* orcid.org/0000-0002-4412-2144; Email: tokeshi@eng.hokudai.ac.jp

Authors

Keine Nishiyama − *Graduate School of Chemical Sciences and Engineering, Hokkaido University, Sapporo 060-8628, Japan;* orcid.org/0000-0002-7433-1019

Masatoshi Maeki − *Division of Applied Chemistry, Faculty of Engineering, Hokkaido University, Sapporo 060-8628, Japan;* orcid.org/0000-0001-7500-4231

Akihiko Ishida − *Division of Applied Chemistry, Faculty of Engineering, Hokkaido University, Sapporo 060-8628, Japan;* orcid.org/0000-0003-4100-9426

Hirofumi Tani − *Division of Applied Chemistry, Faculty of Engineering, Hokkaido University, Sapporo 060-8628, Japan;* orcid.org/0000-0002-5935-0756

Hideaki Hisamoto − *Department of Applied Chemistry, Graduate School of Engineering, Osaka Prefecture University, Osaka, Sakai 599-8531, Japan;* orcid.org/0000-0003-1067-4116

Complete contact information is available at: https://pubs.acs.org/10.1021/acsomega.1c00057

Notes

The authors declare no competing financial interest.

■ ACKNOWLEDGMENTS

K.N. received the Grant-in-Aid for JSPS Fellows 20J11226.

■ REFERENCES

(1) Wu, L.; Qu, X. Cancer Biomarker Detection: Recent Achievements and Challenges. *Chem. Soc. Rev.* **2015**, *44*, 2963−2997.

(2) Sanjay, S. T.; Fu, G.; Dou, M.; Xu, F.; Liu, R.; Qi, H.; Li, X. Biomarker Detection for Disease Diagnosis Using Cost-Effective Microfluidic Platforms. *Analyst* **2015**, *140*, 7062−7081.
(3) Roddam, A. W.; Duffy, M. J.; Hamdy, F. C.; Ward, A. M.; Patnick, J.; Price, C. P.; Rimmer, J.; Sturgeon, C.; White, P.; Allen, N. E. Use of Prostate-Specific Antigen (PSA) Isoforms for the Detection of Prostate Cancer in Men with a PSA Level of 2−10 Ng/Ml: Systematic Review and Meta-Analysis. *Eur. Urol.* **2005**, *48*, 386−399.
(4) Grunnet, M.; Sorensen, J. B. Carcinoembryonic Antigen (CEA) as Tumor Marker in Lung Cancer. *Lung Cancer* **2012**, *76*, 138−143.
(5) Ikami, M.; Kawakami, A.; Kakuta, M.; Okamoto, Y.; Kaji, N.; Tokeshi, M.; Baba, Y. Immuno-Pillar Chip: A New Platform for Rapid and Easy-to-Use Immunoassay. *Lab Chip* **2010**, *10*, 3335−3340.
(6) Han, K. N.; Li, C. A.; Seong, G. H. Microfluidic Chips for Immunoassays. *Annu. Rev. Anal. Chem.* **2013**, *6*, 119−141.
(7) Ali, M. A.; Mondal, K.; Jiao, Y.; Oren, S.; Xu, Z.; Sharma, A.; Dong, L. Microfluidic Immuno-Biochip for Detection of Breast Cancer Biomarkers Using Hierarchical Composite of Porous Graphene and Titanium Dioxide Nanofibers. *ACS Appl. Mater. Interfaces* **2016**, *8*, 20570−20582.
(8) Barbosa, A. I.; Reis, N. M. A Critical Insight into the Development Pipeline of Microfluidic Immunoassay Devices for the Sensitive Quantitation of Protein Biomarkers at the Point of Care. *Analyst* **2017**, *142*, 858−882.
(9) Yamamichi, A.; Kasama, T.; Ohka, F.; Suzuki, H.; Kato, A.; Motomura, K.; Hirano, M.; Ranjit, M.; Chalise, L.; Kurimoto, M.; Kondo, G.; Aoki, K.; Kaji, N.; Tokeshi, M.; Matsubara, T.; Senga, T.; Kaneko, M. K.; Suzuki, H.; Hara, M.; Wakabayashi, T.; Baba, Y.; Kato, Y.; Natsume, A. An Immuno-Wall Microdevice Exhibits Rapid and Sensitive Detection of IDH1-R132H Mutation Specific to Grade II and III Gliomas. *Sci. Technol. Adv. Mater* **2016**, *17*, 618−625.
(10) Nishiyama, K.; Kasama, T.; Nakamata, S.; Ishikawa, K.; Onoshima, D.; Yukawa, H.; Maeki, M.; Ishida, A.; Tani, H.; Baba, Y.; Tokeshi, M. Ultrasensitive Detection of Disease Biomarkers Using an Immuno-Wall Device with Enzymatic Amplification. *Analyst* **2019**, *144*, 4589−4595.
(11) Chávez Ramos, K.; Nishiyama, K.; Maeki, M.; Ishida, A.; Tani, H.; Kasama, T.; Baba, Y.; Tokeshi, M. Rapid, Sensitive, and Selective Detection of H5 Hemagglutinin from Avian Influenza Virus Using an Immunowall Device. *ACS Omega* **2019**, *4*, 16683−16688.
(12) Yogo, N.; Hase, T.; Kasama, T.; Nishiyama, K.; Ozawa, N.; Hatta, T.; Shibata, H.; Sato, M.; Komeda, K.; Kawabe, N.; Matsuoka, K.; Chen-Yoshikawa, T. F.; Kaji, N.; Tokeshi, M.; Baba, Y.; Hasegawa, Y. Development of an Immuno-Wall Device for the Rapid and Sensitive Detection of EGFR Mutations in Tumor Tissues Resected from Lung Cancer Patients. *PLoS One* **2020**, *15*, No. e0241422.
(13) Chen, H.; Fang, Q.; Yin, X.-F.; Fang, Z.-L. Microfluidic Chip-Based Liquid−Liquid Extraction and Preconcentration Using a Subnanoliter-Droplet Trapping Technique. *Lab Chip* **2005**, *5*, 719−725.
(14) Berduque, A.; Zazpe, R.; Arrigan, D. W. M. Electrochemical Detection of Dopamine Using Arrays of Liquid−Liquid Micro-Interfaces Created within Micromachined Silicon Membranes. *Anal. Chim. Acta* **2008**, *611*, 156−162.
(15) Long, Z.; Liu, D.; Ye, N.; Qin, J.; Lin, B. Integration of Nanoporous Membranes for Sample Filtration/Preconcentration in Microchip Electrophoresis. *Electrophoresis* **2006**, *27*, 4927−4934.
(16) Li, F.; Guijt, R. M.; Breadmore, M. C. Nanoporous Membranes for Microfluidic Concentration Prior to Electrophoretic Separation of Proteins in Urine. *Anal. Chem.* **2016**, *88*, 8257−8263.
(17) Wainright, A.; Williams, S. J.; Ciambrone, G.; Xue, Q.; Wei, J.; Harris, D. Sample Pre-Concentration by Isotachophoresis in Microfluidic Devices. *J. Chromatogr. A* **2002**, *979*, 69−80.
(18) Bottenus, D.; Jubery, T. Z.; Ouyang, Y.; Dong, W.-J.; Dutta, P.; Ivory, C. F. 10 000-Fold Concentration Increase of the Biomarker Cardiac Troponin I in a Reducing Union Microfluidic Chip Using Cationic Isotachophoresis. *Lab Chip* **2011**, *11*, 890−898.
(19) Gong, H.; Zhang, B.; Little, G.; Kovar, J.; Chen, H.; Xie, W.; Schutz-Geschwender, A.; Olive, D. M. β-Galactosidase Activity Assay Using Far-Red-Shifted Fluorescent Substrate DDAOG. *Anal. Biochem.* **2009**, *386*, 59−64.
(20) Ishizuka, N.; Hashimoto, Y.; Matsuo, Y.; Ijiro, K. Highly Expansive DNA Hydrogel Films Prepared with Photocrosslinkable Poly(Vinyl Alcohol). *Colloids Surf., A* **2006**, *284−285*, 440−443.
(21) Baptista, J. G. C.; Rodrigues, S. P. J.; Matsushita, A. F. Y.; Vitorino, C.; Maria, T. M. R.; Burrows, H. D.; Pais, A. A. C. C.; Valente, A. J. M. Does Poly(Vinyl Alcohol) Act as an Amphiphilic Polymer? An Interaction Study with Simvastatin. *J. Mol. Liq.* **2016**, *222*, 287−294.
(22) Chang, J. B.; Hwang, J. H.; Park, J. S.; Kim, J. P. The Effect of Dye Structure on the Dyeing and Optical Properties of Dichroic Dyes for PVA Polarizing Film. *Dye. Pigm.* **2011**, *88*, 366−371.
(23) Daina, A.; Michielin, O.; Zoete, V. ILOGP: A Simple, Robust, and Efficient Description of n -Octanol/Water Partition Coefficient for Drug Design Using the GB/SA Approach. *J. Chem. Inf. Model.* **2014**, *54*, 3284−3301.

https://doi.org/10.1021/acsomega.1c00057
ACS Omega 2021, 6, 8340−8345